DOI: 10.4408/IJEGE.2011-03.B-111

THREE-DIMENSIONAL CRITICAL SLIP SURFACE IDENTIFICATION AND SLOPE STABILITY ASSESSMENT OF 11# LAVA LOBE OF UNZEN VOLCANO, JAPAN

Mowen XIE(*), Xiangyu LIU(*), Tetsurou ESAKI(**), Zengfu WANG(*) & Jiehui HUANG(*)

(*)School of Civil and Environmental Engineering, The University of Science and Technology Beijing, Xueyuan Lu 30, Haidian District, Beijing, 100083, China

(**)Research Institute for East Asia Environments,744 Motooka Nishi-ku Fukuoka ,819-0395, Japan

ABSTRACT

Althoug Unzen volcano has been declared to be in a state of relative dormancy, basing on the latcst researchthe latest formed 11# lava lobe now represents a potential slope failure mass. This paper concentrates on the stability of the 11# lava lobe and its possible critical sliding mass. Based on the proposed Geographic Information Systems (GIS) three-dimensional (3D) slope stability analysis models, a 3D locating approach has been used to identify the 3D critical sliding mass and to analyse the 3D stability of 11# lava dome. At the same time, the new 3D approach has shown the effectiveness in selecting the range of the Monte Carlo random variables and in locating the critical slip surface in different parts of the lava dome. The results are very valuable for judging the stability of the lava lobe and for planing the monitoring points.

Key words: *three-dimensional (3D) slope stability, limit equilibrium equation, Unzen volcano, lava lobe, Geographic Information Systems (GIS)*

INTRODUCTION

Unzen volcano, located in Nagasaki prefecture of Japan, abruptly started to erupt after 198 years of dormancy in November 1990 (Yanagi *et alii*, 1994). Following around 8 major incidents up to 1995, it displayed varying aspects of volcanic activities, ranging from early phreatic eruption through to the successive extrusion and growth of lava domes and the formation of pyroclastic flows. However, it has been now, once more, been declared to be in a state of relative dormancy (Yanagi *et alii*, 1994). In these 20 years, the slope failures of lava lobes have been experienced and 44 persons have been killed. Based on the latest research, the latest formed 11# lava lobe now represents a potential slope failure mass. This paper concentrates on the stability of the 11# lava lobe and its possible critical sliding mass.

Presently, the majority of slope stability analyses are performed using a two-dimensional (2D) limit equilibrium method within the domain of geotechnical engineering while the safety factor is commonly assessed using a 2D representation of the slope: for example, an "equivalent" plane-strain problem is postulated and analyzed. The results of the 2D analysis are usually conservative, and although more expensive, the three-dimensional (3D) analysis tends to increase the safety factor. The failure surface is presumed to be infinitely wide in the 2D model, negating the 3D effects caused by the infinite width of the slide mass. Summarized studies concerning 3D slope stability led Duncan (1996) to conclude that the 3D safety factor exceeds that of 2D equivalent, provided that the 2D safety factor is calculated for the most critical 2D section. It will be shown herein that the percentage difference between the 2D and 3D analyses may be as large as 30% (the difference is between around 3%-30% with an average is 13.9%; Gens *et alii*, 1988), and thus a 3D analysis is the preferred means of con-

ducting slope stability analyses.

Since the mid-1970s, the development and application of 3D stability models (DUNCAN, 1996) has attracted growing interest. However, although several 3D methods of analysis have been proposed in geomechanical literature (XIE *et alii*, 2003a; CHEN *et alii*, 2003), a practical 3D slope stability analysis method and related computer programs are still urgently required.

In this study, as a new contribution and a follow up to former research (XIE *et alii*, 2003a; 2003b; 2004a; 2004b), the Geographic Information Systems (GIS) grid-based data is analyzed with four proposed column-based 3D slope stability analysis models (XIE *et alii*, 2003b; HUNGR *et alii*, 1989) and the correspondent new GIS grid-based 3D deterministic models will be applied in order to calculate the safety factors. At the same time, a new developed GIS-based program, 3DSlopeGIS, will be used to evaluate the 3D stability of the 11# complicated lava lobe of Unzen volcano (YANAGI *et alii*, 1994). This practical application of the 3D slope stability assessment will illustrate the effectiveness of 3DSlopeGIS in selecting the range of the Monte Carlo random variables and in locating the critical slip surface of the lava dome.

GIS GRID-BASED 3D MODELS AND CRITICAL SLIP SURFACE LOCATING

Using the functions of the GIS spatial analysis, all input data (such as elevation, inclination, slope, groundwater, strata, slip surface and mechanical parameters) for the safety factor calculation are available with respect to each grid pixel, while all slope-related data are grid-based. Figure 1 shows a real slope mass and its abstracting GIS layers. In GIS, the reality of a landslide is abstracted to GIS layers for each topographic and geological theme, each layer of which represents each theme: ground surface, strata, weak discontinuities, groundwater and slip surface, respectively. By inputting these data into a deterministic model of slope stability, a safety factor value is calculated.

In this study, combining the GIS grid-based data with four proposed column-based 3D slope stability analysis models, their GIS grid-based 3D deterministic models is deduced to calculate safety factor:

1) the first one is based on HOVLAND's model (1977);
2) the second one is based on the algorithm of the 3D stability analysis method proposed by HUNGR (1987): it is a 3D extension of BISHOP (1954) 2D model, it allows to consider conside the differenttypes of slip surface ,and has been widely addressed in geotechnical literatures (HUNGR, 1987; HUNGR *et alii*, 1989).
3) the third one is also based on the work of HUNGR *et alii* (1989): this model is an extension of Janbu's simplified 2D method, deduced from the horizontal forces equilibrium equation along the slip direction.
4) The fourth model is based on the assumption of HOVLAND's model (1977). The basic algorithm is based on a former research (XIE *et alii*, 2003a; 2003b) in which the external load and the seismic load are considered.

The first and the fourth methods assume that the vertical sides of each pixel column are frictionless and can be used for any shape slip surface. The second method is based on two assumptions:

1. the vertical shear force acting on both the longitudinal and lateral vertical faces of each grid-column can be neglected in the equilibrium equation
2. the vertical force equilibrium equation of each grid-

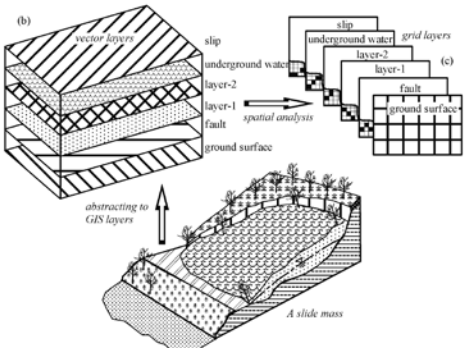

Fig. 1 - A slope failure mass and its abstracted GIS layers

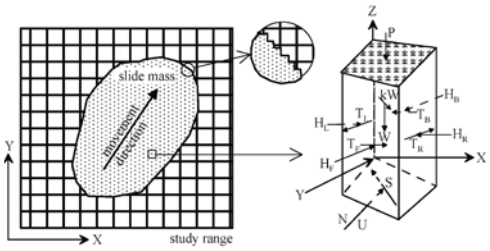

Fig. 2 - A slope failure mass and forces acting on a single grid-column

column and the summary moment equilibrium equation of the entire assemblage of grid-column are sufficient conditions to determine all of the unknown forces.

Then, this method can only be used for rotation surface. The third one can be deduced from the horizontal forces equilibrium equation and then can be used for any shape slip surface.

Refer to the first method- Using the pixels in the range of sliding mass, the 3D safety factor is deduced by force and/or moment equilibrium of each pixel-column (Fig. 2). The equation of HOVLAND's (1977) model is deduced to GIS grid form as following (XIE *et alii*, 2003a):

$$SF_{3D}=\frac{\sum_J\sum_I\{c'A+[(W+P)\cos\theta-U]\tan\phi'\}}{\sum_J\sum_I[(W+P)\sin\theta_{Avr}+kW]-E} \quad (1)$$

Refer to the secon method- With reference to Fig. 2, considering the equilibrium equation of the vertical force of one grid-column, the following equation can be obtained:

$$N=\frac{P+W+QU-Rc'}{\cos\theta+Q} \quad (2)$$

$$Q=SF_{3D}^{-1}\tan\phi'\sin\theta_{Avr} \qquad R=SF_{3D}^{-1}A\sin\theta_{Avr}$$

Then, the equation for calculating the 3D safety factor is deduced as the Bishop 3D extending model (HUNGR, 1987):

$$SF_{3D}=G\sum_J\sum_I\frac{(W+P-U\cos\theta)\tan\phi'+c'A\cos\theta}{\cos\theta+Q} \quad (3)$$

$$G=(\sum_J\sum_I(W+P)\sin\theta_{Avr})^{-1}$$

Because the SF_{3D} is implicit in equation(3), the safety factor SF_{3D} is calculated using equations(2) and (3) by an iterative procedure. Refer to the third method, a 3D equivalent of the Janbu simplified method without a correction factor can be deduced from the horizontal forces equilibrium equation along the slip direction (HUNGR *et alii*, 1989):

$$SF_{3D}=\frac{\sum_J\sum_I[c'A+(N-U)\tan\phi']\cos\theta_{Avr}}{\sum_J\sum_I(N\sin\theta\cos(Asp-AvrAsp)+kW)-E} \quad (4)$$

The safety factor SF_{3D} is calculated using equations (2) and (4) by an iterative procedure

Using the grid database of surface (XIE *et alii*, 2003a; 2003b), strata, groundwater, fault and slip surface, a GIS grid-based equation, all the resistant and sliding forces refer to the possible sliding direction, but not necessary to the Y-axis direction that is used in HOVLAND's model (1977).

$$SF_{3D}=\frac{\sum_J\sum_I\{c'A+[(W+P)\cos\theta-U]\tan\phi'\}\cos\theta_{Avr}}{\sum_J\sum_I[(W+P)\sin\theta_{Avr}\cos\theta_{Avr}+kW]-E} \quad (5)$$

where, SF_{3D} = the 3D slope safety factor; W = the weight of one column; A = the area of the slip surface; c' = the effective cohesion; Φ' = the effective friction angle; θ = the dip (the normal angle of slip surface); and J , I = the numbers of row and column of the grid in the range of slope failure (in this study, a polygon feature will be used to confine the boundary of the slide mass); U is the pore pressure acting on the slip surface of each column; P is the vertical force acting on each column (the distributed force of upper load); k is the horizontal earthquake acceleration factor; E is the resultant of all horizontal components of applied point loads, the reinforcement force is considered in this force.

For each methods indicated before,the most critical situations have been investigated,by means of minimization of the 3D safety factor using the Monte Carlo random simulation method for detecting the 3D critical slip. The initial slip surface is assumed as the lower part of an ellipsoid slip, then each randomly produced slip surface is changed according to the different stratum strengths and conditions of weak discontinuities. Finally, the critical slip surface is obtained and consequently a relative minimization of the

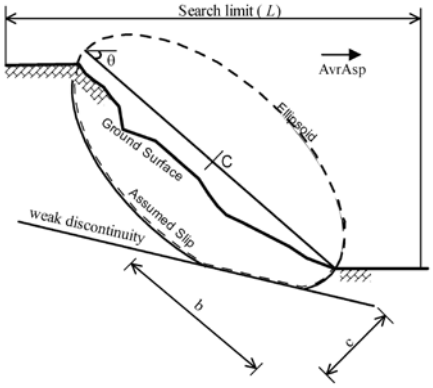

Fig. 3 - Assumed slip surface and calculation parametrs

3D safety factor is achieved (XIE *et alii*, 2004b).

The critical slip surface is obtained by means of a trial searching and 3D safety factor calculation, in which, the five parameters, of size and posture of the ellipsoid, are selected as random variables for Monte Carlo simulating: three axial parameters " *a,b,c* ", the central point *"C"* and the inclination angle "θ " of the ellipsoid. If a randomly produced slip surface based on the lower part of an ellipsoid is lower than a weak discontinuous surface or the confines of the hard stratum, the weak discontinuity or the confine surface of the hard stratum will be given priority for being selected as one part of the assumed slip surface. Figure 3 shows an assumed slip surface is composed of one part of the ellipsoid and one part of the weak discontinuity.

The geometrical parameters, *a,b,c* of the ellipsoid, are randomly selected in a certain range that is set as in Equation (1):

$$\begin{aligned} a &\in (a_{\min}, a_{\max}) \\ b &\in (b_{\min}, b_{\max}) \\ c &\in (c_{\min}, c_{\max}) \end{aligned} \tag{6}$$

The central point *"C"* of the ellipsoid is first set to be the centroid of the search limit or a researcher-selected point, and then in each trial searching, random walking will change the central point.

The inclination direction of the ellipsoid is set to be the same as the direction of the slope, and the inclination angle θ of the ellipsoid is basically set according to the slope angle. If a slope has complicated topographic characteristics, the inclination parameter of an ellipsoid is set to the main inclination of the slope as shown in Fig. 4.

The five parameters, three axial parameters "*a,b,c*", the central point *"C"* and the inclination angle *"θ "* of the ellipsoid, are selected as the random variables for Monte Carlo simulatingin the range of [0,1]

The random variable of a uniform distribution within the range of [0,1] is obtained by the method of multiplicative congruity:.

$$\begin{aligned} y_i &= a y_{i-1} Mod(m) \\ r_i &= y_i / m \end{aligned} \tag{7}$$

where a = a constant of positive integer; m = the module; r_i = the random variable of the uniform distribution within the range of [0,1]; by setting an initial value of y_0 , each random variable r_i can be obtained. The random variable within the range of is then calculated by Equation (8),

$$x_i = r_i(b-a) + a \tag{8}$$

where x_i = the random variable within the range of [a,b].

3D SLOPE STABILITY ASSESSMENT OF 11# LAVA LOBE OF UNZEN VOLCANO

BASIC INFORMATION AND GIS DATA PROCEEDING

Unzen volcano is located in Nagasaki prefecture of Ja-

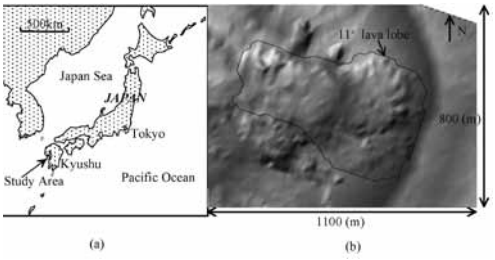

Fig.5 - The Unzen volcano and its location

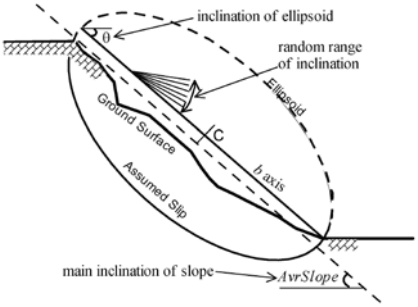

Fig. 4 - The inclination of ellipsoid and slope

Fig. 6 - 11# lava lobe of the Unzen volcano (east viewpoint)

pan (Fig. 5a). In this study, we select the latest formed 11# lava lobe as study object (Fig. 5b) for evaluating the stability of the 11# lava lobe and for locating the critical slip surface. Fig. 6 shows a photo of the 11# lava lobe of volcano lava.

The topographic data are calculated using aerial photography, and comparing the difference in such photos before and after each eruption allows each lava lobe to be detected, and at the same time, the topographical data for each occasion to be determined. The 11# lava lobe was formed between Apr. 1993 and Apr.1994, and its shape can be revealed from comparison between two aerial photos taken in Feb.1993 and Sept.1994 respectively, revealing the 3D shape of the 11# lava lobe. The DEM data on each occasion, meanwhile, is deduced from the aerial photo by means of the following steps:

1) Selecting datum: using local triangle net and level points;
2) Triangle measure: air triangle surveying;
3) Grid measure: in the range of 1200 m × 1700 m, the X, Y, and Z values of each grid are obtained (the grid size is 20 m and the DEM precision elevation is in centimeter. please indicate the DEM precision in elevation);
4) Digital photos georeference: georeferencing the air photos and corresponding to the actual site;
5) Coordinate conversion: changing to a common coordinate system;
6) Forming TIN and converting into grid data: converting the TIN dataset to a grid raster dataset.

The ground surfaces of each eruption are then abstracted as a GIS grid dataset. The adjacent interface is considered as the possible sliding surface, then the interface of two lava lobes in Feb.1993 and Sept.1994, as a weak layer, is considered as a possible slip surface and the geomechanical parameters of the lava layer and interface are listed in Table 1.

SUITABLE RANDOM VARIABLE SELECTION IN MONTE CARLO SIMULATION

The basic Monte Carlo simulation method has been detailed in a former research paper (Xie *et alii*, 2004b), and here the method will be applied to this practice problem in order to detect the critical slip surface and the sliding bodies respectively.

	c (kN/m^2)	φ(°)	γ (kN/m^3)
Lava layer	1500	30	22.1
Interface	140	32.9	/

Tab. 1 - The geomechanical parameters

For the critical slip identification, a test for the suitable Monte Carlo random calculating time is performed; with a trial calculation frequency of up to 1000 times. The resultant minimum 3D safety factors of each trial calculation are illustrated in Fig. 8. For this case, considering the time consumed and effectiveness, the minimum safety factor can be obtained following around 300 trial calculations. In the following random variables studies, the calculating time for the Monte Carlo simulation is set at 300 times.

In a former study (Xie *et alii*, 2004b), for explaining the relationship of the ratio of *a / b* (the width and length of the ellipsoid) and the critical 3D safety factor, different *a / b* ratios are selected to locate the critical slip and calculate the 3D safety factor. When the ratio of *a / b* is smaller than 0.8, the 3D safety factor will increase sharply corresponding to the decreased *a / b* ratio. Conversely, if the ratio of *a / b* exceeds

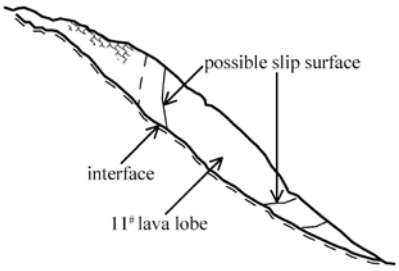

Fig. 9 - Relationship between the minimum safety factor and the a / b ratio

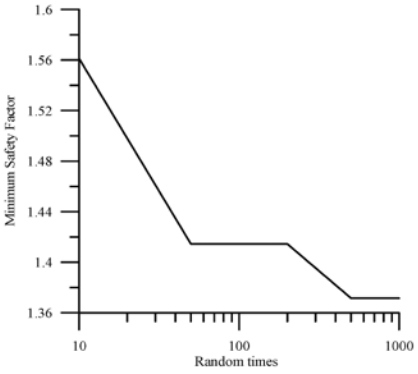

Fig. 8 - Resultant minimum safety factor and random Monte Carlo calculating times

0.8, the 3D safety factor will decrease slowly with an increase in the *a / b* ration until finally, the 3D safety factor will approach the 2D safety factor (with the increase in the ratio of *a / b* , the problem of 3D safety factor calculation approaches the plain-strain assumption that is used to calculate the 2D safety factor).

In this application study, the relationship of a / b and the minimum safety factor has been studied based on two conditions (Fig. 9). is maintained in the same range, with the increasing values of *a / b* , the minimum safety factor will increase. However, in the case of the same b, with increasing values of *a / b* , the minimum safety factor will decrease, since the random selected sliding mass will approach a 2D case (Xie *et alii*, 2004b). This study reveals that the *a / b* ratio of around 0.5-0.6 will be a suitable ratio for effectively locating the critical slip surface.

When calculating the 3D safety factor, the force and moment equations for each column are based on the value of *AvrAsp* the average dip direction is assumed as the sliding direction). To confirm this assumption, the different range of *AvrAsp* were studied in this application study. For one case of *AvrAsp = 90*, the ranges of dip direction (aspects) were selected as 89~91, 80~100 and 70~110 respectively, and their minimum safety factors 1.415,1.437 and 1.490 respectively. At the same time, three cases provided a broadly similar critical slip surface and with the same critical direction (about 90 degrees). This comparative study can confirm the assumptions of "*AvrAsp* = sliding direction".

A suitable range for the dip (slope angle) has also been studied. For one case of *AvrSlope=33.5*, the ranges are set to be 25~40, 25~33.5 and 33.5~40 respectively, with resulting minimum safety factors of 1.412, 1.455 and 1.406 respectively. At the same time, using *AvrSlope*±10%, ±20%, ±30%, ±40%, the corresponding results are 1.412, 1.407, 1.409, and 1.407 respectively. This result indicates that more than ±20% range set cannot result a lower safety factor. Then, we set the range of *AvrSlope*±20% for effectively locating the critical slip surface.

In the Monte Carlo simulation, each central point of the ellipsoid was randomly selected around the start point. As shown in Fig.10, the randomly selected central points are around a start point. At the same time, we found that the different start points result different minimum safety factors which are depending on the geological structure and the topographic conditions. This means that prior to the calculation, the geological engineering and topographic conditions had to be carefully studied to determine a suitable start point.

The resultant minimum safety factor and calculation time have also been compared using different 3D models. For certain case study, the differences are illustrated in Table 2. It can be seen that there is no apparent difference in the calculation time because of the same data management for different models, while the iterative proceeding for the Bishop and Janbu 3D extension

3D models	Hovland	Bishop extension	Janbu extension
Calculating time (sec./1000 times)	1074	1116	1168
Minimum safety factor	1.24245	1.371614	1.321941

Tab. 2 - Calculating time and minimum safety factors for different models

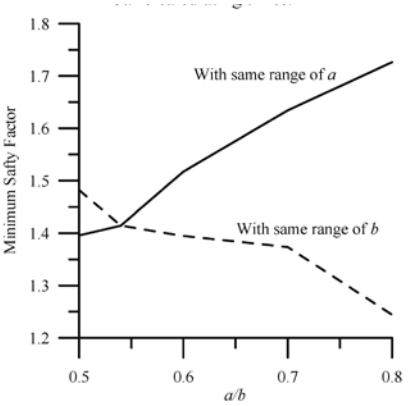

Fig. 10 - The start point and random central points in the Monte Carlo simulation

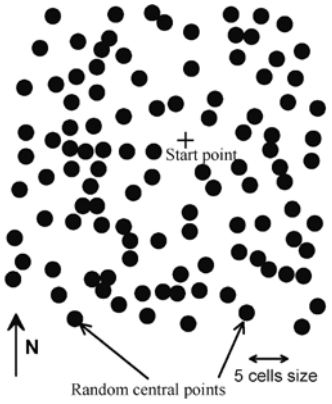

Fig. 10 - The start point and random central points in the Monte Carlo simulation

models takes a little more time. On the other hand, because it neglects the interactive forces of the column, Hovland's model results in the lowest safety factor.

OVERALL AND PARTIAL STABILITY OF 11# LAVA LOBE OF UNZEN VOLCANO

For evaluating the 3D stability of 11# lava lobe comprehensively, 4 scenarios are selected to identify the 3D critical sliding masses. In Fig.11,sliding volum A is used to assess the possible slope failure of the 11# lava lobe as a whole. At the same time,B, C and D are set to analyzing the critical sliding masses of the front toe of the 11# lava lobe. Theses 4 sliding volume scenarios assures that the different sityationsbe considered in the 11# lava lobe.

Taking the 11# lava lobe as a whole, varying cases with a range of different random variables have been calculated. The section of resultant critical sliding mass is illustrated in Fig.12a (with a 3D view shown in Fig.12b), and the minimum safety factors are revealed as 1.322, 1.388 and 1.346 using Hovland's, Bishop and Janbu 3D extension models respectively; considering the possible influence of earthquake with the horizontal coefficient of k =0.05, the 3D safety factors will be 1.162, 1.235 and 1.159 respectively.

The former study of the sliding patterns concluded that the front toe of the 11# lava lobe is relatively unstable (YANAGI *et alii*, 1994). Therefore, in this study, the relative potential of a minor slope failure in the front toe section was studied too, Fig.13,14 and 15 represent the section and the 3D view of the critical sliding masses in range B,C, and D respectively. The resultant minimum safety factors are 1.508, 1.531 and 1.509 in the north (D), mid (B) and south (C) sections of the toe respectively. Considering the possible vertical cracks cutting through the 11# lava lobe, the minimum safety factors would be 1.012, 1.221 and 1.210 respectively. At the same time, the same earthquake with the horizontal coefficient of k =0.05 will result the 3D minimum safety factors of 1.322, 1.351 and 1.300 respectively.

Finally, the following conclusions can be obtained from the stability study of the 11# lava lobe of Unzen volcano:

1) The study shows the 11# lava lobe is now in a stable condition based on the proposed geomechanical parameters(discuss this point not considering the influence of earthquake);
2) A trial study is necessary to set a suitable range of

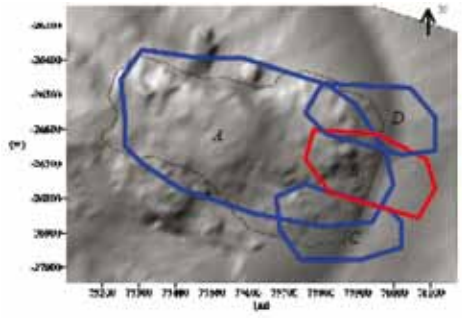

Fig. 11 - The searching ranges for locating critical sliding masses

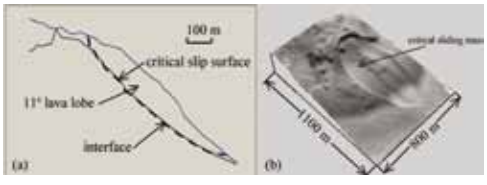

Fig. 12 The section and 3D view of a critical sliding mass in range A

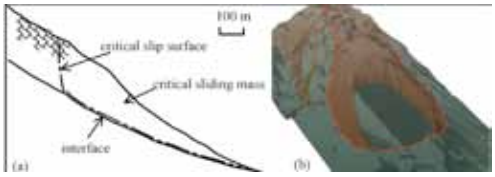

Fig. 13 - The section and 3D view of a critical sliding mass in range B

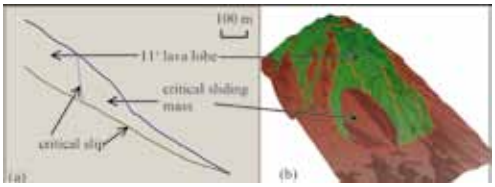

Fig. 14 - The section and 3D view of a critical sliding mass in range C

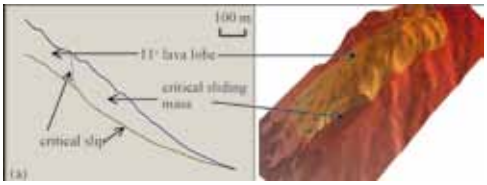

Fig. 15 - The section and 3D view of a critical sliding mass in range D

random variables to effectively identify the critical slip surface;

3) If the possible vertical cracks are considered, the front toe of the 11# lava lobe will be considered in a dangerous condition;
4) Moreover, if any slope failure in the front toe takes place, the whole stability of 11# lava lobe will be affected too.

CONCLUSIONS

Combining the GIS grid-based data with four proposed column-based 3D slope stability analysis models, the slope stability of Unzen volcano lava lobe has been evaluated and the results have illustrated the convenience in the data management, in the effectively selecting the range of the Monte Carlo random variables, and in licating the critical slip surface. These results will be a valuable reference for taking measures against the slope failure hazard and for setting the monitoring equipments.

Benefiting from the convenient functions of data management and the GIS spatial analysis, the new database approach will present a new challenge for the geotechnical researchers using traditional numerical methods for 3D slope stability assessment.

ACKNOWLEDGMENTS

The authors are most grateful for the funding support for this research provided by JSPS and Sabo Technical Center, Japan.

REFERENCES

Bishop A.W. (1954) - *The use of the slip circle in the stability analysis of slopes*. Geotechnique, **5**(1)**:** 7-17.

Chen Z., Mi H., Zhang F. & Wang X. (2003) - *A simplified method for 3D slope stability analysis*. Canadian Geotechnical Journal 2003; **40:** 675-683.

Duncan J.M. (1996) - *State of the art: limit equilibrium and finite-element analysis of slopes.* Journal of Geotechnical and Geoenvironmental Engineering ASCE, **122**(7)**:** 577-596.

Gens A., Hutchison J.N. & Cavounidis S. (2003) - *Three dimensional analysis of slices in cohesive soils.* Geotechnique, **38:** 1-23.

Hovland H.J. (1977) - *Three-dimensional slope stability analysis method.* Journal of the Geotechnical Engineering, Division Proceedings of the American Society of Civil Engineers, **103**(GT9): 971-986.

Huang C.C., Tsai C.C. (2000) - *New method for 3D and asymmetrical slope stability analysis.* Journal of Geotechnical and Geoenvironmental Engineering, ASCE, **126**(10)**:** 917-927.

Huang C.C., Tsai C.C., Chen Y.H. (2002) - *Generalized Method for Three-Dimensional Slope Stability Analysis.* Journal of Geotechnical and Geoenvironmental Engineering, ASCE, **128**(10): 836-848.

Hungr O. (1987) - *An extension of Bishop's simplified method of slope stability analysis to three dimensions.* Geotechnique, **37**(1)**:** 113-117.

Hungr O., Salgado F.M., Byrne P.M. (1989) - *Evaluation of a three-dimensional method of slope stability analysis.* Canadian Geotechnical Journal, **26**: 679-686.

Lam L. & Fredland D.G. (1993) - *A general limit equilibrium model for three-dimensional slope stability analysis*. Canadian Geotechnical Journal, **30:** 905-919.

Xie M., Esaki T., Zhou G. Mitani Y. (2003a) - *Three-dimensional stability evaluation of landslides and a sliding process simulation using a new geographic information systems component*. Environmental Geology, **43:** 503-512.

Xie M., Esaki T., Zhou G. & Mitani Y. (2003b) - *Geographic information systems-based three-dimensional critical slope stability analysis and landslide hazard assessment.* ASCE, Journal of Geotechnical and Geoenvironmental Engineering, **129**(12)**:** 1109-1118.

Xie M., Esaki T. & Zhou G. (2004a) - *Three-dimensional stability evaluation of landslides and a sliding process simulation using a new geographic information systems component*. Natural Hazards, **43:** 503-512.

Xie M., Esaki T. & Cai M. (2004b) - *A GIS-based method for locating the critical 3D slip surface in a slope*. Computers and Geotechnics, **31:** 267-277.

Yanagi T., Okada H., & Ohta K. (1994) - *Unzen Volcano: the 1990-1992 eruption*. The Nishinippon & Kyushu University Press, Fukuoka, Japan.